ELSEVIER

Fluid Phase Equilibria 142 (1998) 253–280

FLUID PHASE EQUILIBRIA

Transport properties of carbon dioxide + ethane and methane + ethane mixtures in the extended critical region [1]

S.B. Kiselev *, M.L. Huber

Physical and Chemical Properties Division, National Institute of Standards and Technology, 325 Broadway, Boulder, CO 80303, USA

Received 3 March 1997; accepted 27 August 1997

Abstract

A practical representation for the transport coefficients of pure fluids and binary mixtures in and beyond the critical region of liquid-vapor equilibria is presented. The crossover expressions for the thermal conductivity, the binary diffusion coefficient, the thermal diffusion coefficient, and the thermal diffusion ratio incorporate scaling laws near the critical point and are transformed to regular background values far away from the critical point. In the limits of pure components, the crossover expression for the thermal conductivity of binary mixtures is transformed to the crossover expression for the thermal conductivity of pure fluids. For the calculation of the regular backgrounds transport properties of pure fluids, we use dense fluid contributions obtained from independently fitting pure fluid data and a dilute gas contribution from Chapman–Enskog theory. A comparison is made with thermal conductivity data for pure carbon dioxide, methane, ethane, and carbon dioxide + ethane and methane + ethane mixtures. © 1998 Elsevier Science B.V.

Keywords: Binary mixtures; Carbon dioxide; Critical state; Diffusion coefficient; Ethane; Methane; Thermal conductivity

1. Introduction

It is well known that both the thermodynamic surface and the transport properties of fluids exhibit singularities at the critical point [1,2]. Asymptotically close to the critical point the singular behavior of transport coefficients in pure fluids and in binary mixtures can be described in terms of scaling laws with universal exponents and universal scaling functions [3–7]. On the other hand, far away from the critical point, the intensity of the critical fluctuations is diminished and the thermodynamic

* Corresponding author. Institute for Oil and Gas Research of the Russian Academy of Sciences, Leninsky Prospect 63/2, Moscow 117917, Russian Federation.

[1] Contribution of the National Institute of Standards and Technology, not subject to copyright in the United States.

PII S0378-3812(97)00222-7

and transport properties of fluids can be described in terms of regular analytical equations. In order to describe the transport properties of fluids and fluid mixtures in the wide region of temperatures and densities around the critical point, it is necessary to consider the nonasymptotic critical behavior of the thermodynamic and transport properties including the crossover to regular classical behavior far from the critical point. In the last several years, significant progress in the description of the transport coefficients of binary mixtures in and beyond the critical region has been achieved. The decoupled-mode calculations by Kiselev and coworkers [8–11], the renormalization group calculations by Folk and Moser [12–14], and the recent mode-coupling results obtained by Luettmer-Strathmann and Sengers [15] not only confirm earlier asymptotic predictions, but also extend the description of the transport properties of binary mixtures into the crossover region. These studies show that in order to extend this crossover approach for the transport coefficients in binary mixtures to the entire thermodynamic surface, special attention has to be paid to the equation of state and to the regular background contributions of the kinetic coefficients.

The present paper provides a practical representation of transport properties of binary mixtures in and beyond the critical region based on the modern theory of critical phenomena. We calculate the thermodynamic properties of pure fluids and binary mixtures using a new parametric crossover equation of state, which incorporates scaling laws asymptotically close to the critical point and transforms into the regular classical expansion far away from the critical point [16,17]. In evaluating the crossover expressions for the kinetic coefficients in binary mixtures, we use the decoupled-mode calculations of Kiselev and Kulikov [8,11]. The correct regular behavior of the transport coefficients is provided by the redefinition of the correlation length of the order–parameter fluctuations. In the vicinity of the critical point the crossover expression for the critical enhancement of the transport coefficients in a binary mixture incorporate the scaling laws and reproduce the asymptotic expressions obtained earlier by Mistura [4,5]. Far away from the critical point the crossover expressions transform into their regular background parts.

We proceed as follows. In Section 2, we formulate the crossover equations for the transport coefficients. In Section 3, we propose corresponding states expressions for calculating the regular (background) parts of the kinetic coefficients in binary mixtures; a comparison with experimental thermal conductivity data for pure carbon dioxide, methane and ethane is given in Section 4. In Section 5, we compare our crossover model with experimental thermal conductivity, thermal and binary diffusion, and thermodiffusion ratio data for carbon dioxide + ethane and methane + ethane methane mixtures. In Section 6, we discuss our results.

2. Crossover equations for the transport coefficients

The Onsager expressions for the diffusion current $\vec{J}_d$ and heat current $\vec{J}_q$ in binary mixtures are [18]

$$\vec{J}_d = -\tilde{\alpha}\vec{\nabla}\mu - \tilde{\beta}\vec{\nabla}T \tag{1}$$

$$\vec{J}_q = -\tilde{\beta}T\vec{\nabla}\mu - \tilde{\gamma}\vec{\nabla}T + \mu\vec{J}_d \tag{2}$$

where T is the temperature, $\mu = \mu_2 - \mu_1$ is the chemical potential of the mixture, and $\tilde{\alpha}$, $\tilde{\beta}$ and $\tilde{\gamma}$

are Onsager kinetic coefficients. Mode-coupling calculations performed by Gorodetskii and Giterman [3] and Mistura [4,5] show that asymptotically close to the critical point the Onsager kinetic coefficients diverge as

$$\Delta\tilde{\alpha} = \tilde{\alpha} - \tilde{\alpha}_b = \frac{k_B T\rho}{6\pi\eta\xi}\left(\frac{\partial x}{\partial \mu}\right)_{P,T} \tag{3}$$

$$\Delta\tilde{\beta} = \tilde{\beta} - \tilde{\beta}_b = \frac{k_B T\rho}{6\pi\eta\xi}\left(\frac{\partial x}{\partial T}\right)_{P,\mu} \tag{4}$$

$$\Delta\tilde{\gamma} = \tilde{\gamma} - \tilde{\gamma}_b = \frac{k_B T\rho}{6\pi\eta\xi}\left(\frac{\partial S}{\partial T}\right)_{P,\mu} \tag{5}$$

where η is the shear viscosity, ρ the density, $x = N_2/(N_1 + N_2)$ the mole fraction of the second component, S the molar entropy of the mixture, ξ the equilibrium correlation length, k_B Boltzmann's constant, and where the subscript 'b' denotes the background part of the kinetic coefficients which is an analytic function of the concentration, temperature and density. The asymptotic equations, Eq. (3)–Eq. (5), are valid only in an extremely small range of temperatures and densities around the critical point. In order to describe the behavior of the transport coefficients of binary mixtures in the entire range of temperatures and densities, including the critical region, the crossover expressions for the kinetic coefficients $\tilde{\alpha}$, $\tilde{\beta}$ and $\tilde{\gamma}$ have to be used. In the present paper for the calculations of the transport coefficients in pure components and in binary mixtures we use the decoupled-mode results obtained by Kiselev and Kulikov [8,11]. In this approach the crossover expressions for the kinetic coefficients of a binary mixture are written in the form

$$\tilde{\alpha} = \frac{k_B T\rho}{6\pi\eta\hat{\xi}}\left(\frac{\partial x}{\partial \mu}\right)_{P,T} \Omega_\alpha\left(q_D\hat{\xi}\right) + \tilde{\alpha}_b \tag{6}$$

$$\tilde{\beta} = \frac{k_B T\rho}{6\pi\eta\hat{\xi}}\left(\frac{\partial x}{\partial T}\right)_{P,\mu} \Omega_\alpha\left(q_D\hat{\xi}\right) + \tilde{\beta}_b \tag{7}$$

$$\tilde{\gamma} = \frac{k_B T^2\rho}{6\pi\eta\hat{\xi}}\left(\frac{\partial x}{\partial \mu}\right)_{P,T}\left(\frac{\partial \mu}{\partial T}\right)^2_{P,x} \Omega_\alpha\left(q_D\hat{\xi}\right) + \frac{k_{FUNCZB} T\rho C_{P,x}}{6\pi\eta\hat{\xi}}\Omega\left(q_D\hat{\xi}\right) + \tilde{\gamma}_b \tag{8}$$

where the crossover functions $\Omega_{\hat{\alpha}}(q_D\hat{\xi})$ and $\Omega(q_D\hat{\xi})$ are given by equations

$$\Omega_\alpha\left(q_D\hat{\xi}\right) = \frac{2}{\pi}\left[\arctan\left(q_D\hat{\xi}\right) - \frac{1}{\sqrt{1 + y_D q_D\hat{\xi}}}\arctan\frac{q_D\hat{\xi}}{\sqrt{1 + y_D q_D\hat{\xi}}}\right] \tag{9}$$

$$\Omega\left(q_D\hat{\xi}\right) = \frac{2}{\pi}\left[\arctan\left(q_D\hat{\xi}\right) - \frac{1}{\sqrt{1 + y_{1D} q_D\hat{\xi}}}\arctan\frac{q_D\hat{\xi}}{\sqrt{1 + y_{1D} q_D\hat{\xi}}}\right] \tag{10}$$

with

$$y_D = \frac{6\pi\eta^2}{k_B T\rho q_D\left(\phi_0 + \gamma_0^{-1}\right)} \tag{11}$$

$$y_{1D} = \frac{6\pi\eta^2}{k_B T \rho q_D (\phi_0 + y_1^{-1})} \tag{12}$$

where

$$y_0 = \frac{k_B T \rho}{6\pi\eta\hat{\xi}\tilde{\alpha}_b}\left(\frac{\partial x}{\partial \mu}\right)_{P,T} \tag{13}$$

and

$$y_1 = \frac{k_B T^2 \rho}{6\pi\eta\hat{\xi}\tilde{\gamma}_b}\left(\frac{\partial S}{\partial T}\right)_{P,\mu} \tag{14}$$

In Eq. (6)–Eq. (14), $q_D = |\vec{q}_D|$ is a cutoff wave number first introduced by Perl and Ferrell [19,20], and $\phi_0 = \phi(k_D\hat{\xi})$ is the dynamical scaling function

$$\phi(z) = \Omega_K(z)/(1+z^2) \tag{15}$$

(where $\Omega_K(z) = (3/4z^2)[1 + z^2 + (z^3 - z^{-1})\arctan(z)]$ is the Kawasaki function [21–24]) calculated at the constant value of the wave number $k_D = 0.1 q_D$. Eq. (6)–Eq. (14) coincide with the corresponding expressions obtained by Kiselev and Kulikov [8,11]; however unlike Refs. [8,11], in the present work we define the renormalized correlation length as

$$\hat{\xi} = \xi_{OZ} \exp\left(-\frac{1}{q_D \xi_{OZ}}\right) \tag{16}$$

where

$$\xi_{OZ} = \xi_0 \sqrt{\frac{\tilde{\chi}}{\Gamma_0}} \tag{17}$$

corresponds to the Ornstein–Zernike approximation for the correlation length, ξ_0 and Γ_0 are the amplitudes of the asymptotic power laws for the correlation length and reduced isomorphic compressibility $\tilde{\chi} = \rho(\partial\rho/\partial P)_{T,\mu} P_c \rho_c^{-2}$, respectively. Asymptotically close to the critical point $q_D\hat{\xi} \gg 1$, the singular parts of the kinetic coefficients are much larger than the regular (background) parts ($y_0 \gg 1$, $y_1 \gg 1$, $y_D \approx y_{1D} \approx 1$), all crossover functions approach unity, and Eq. (6)–Eq. (8) in the critical limit reduce to the asymptotic solution given by Eq. (3)–Eq. (5). Far away from the critical point, i.e., $q_D\hat{\xi} \ll 1$, the crossover functions tend to zero ($\Omega_\alpha \to 0$; $\Omega \to 0$), and all kinetic coefficients approach their regular parts. Thus with the definition Eq. (16), q_D^{-1} has the meaning of a statistical average distance at which the real correlation length becomes e times less then the Ornstein–Zernike correlation length Eq. (17), and where, as a consequence, the decoupled-mode calculations cannot be applied anymore.

The thermal conductivity of the mixture λ is defined by the equations [18]

$$\vec{J}_d = 0, \vec{J}_q = -\lambda\vec{\nabla}T \tag{18}$$

which according to Eq. (6)–Eq. (8) lead to the following expression for the thermal conductivity of binary mixtures [8,11]

$$\lambda = \tilde{\gamma} - T\frac{\tilde{\beta}^2}{\tilde{\alpha}} = \frac{k_B T \rho C_{P,x}}{6\pi\eta\hat{\xi}}\Omega\left(q_D\hat{\xi}\right) + \tilde{\alpha}_b \mu_T^2 T Q(y) + \tilde{\gamma}_b \tag{19}$$

where the crossover function $\Omega_\alpha(q_D\hat{\xi})$ appears only in the argument

$$y = \Delta\tilde{\alpha}/\tilde{\alpha}_b = y_0\Omega_\alpha\left(q_D\hat{\xi}\right) = \frac{k_B T\rho}{6\pi\eta\hat{\xi}\tilde{\alpha}_b}\mu_x^{-1}\Omega_\alpha\left(q_D\hat{\xi}\right) \tag{20}$$

of the function

$$Q(y) = \frac{y(1+2y^*) - (y^*)^2}{1+y} \tag{21}$$

Here we have introduced the notation $\mu_x = (\partial\mu/\partial x)_{P,T}$, $\mu_T = (\partial\mu/\partial T)_{P,x}$, and $y^* = \tilde{\beta}_b/\mu_T\tilde{\alpha}_b$. In the limit of pure components ($x \to 0$ or $x \to 1$), $\tilde{\alpha}_b \sim x(1-x) \to 0$ [7,8], the specific heat capacity $C_{P,x}$ of a binary mixture is transformed to the isobaric specific heat capacity C_P of the pure components, and Eq. (19) for the thermal conductivity of the binary mixtures transforms to the crossover equation for the thermal conductivity of the one-component fluid.

In order to calculate the thermo- and barodiffusivity we represent the diffusion current in the form [18]

$$\vec{J}_d = -\rho D_{12}\vec{\nabla}x - \frac{\rho D_T}{T}\vec{\nabla}T - \frac{\rho D_P}{P}\vec{\nabla}P \tag{22}$$

where the binary diffusion coefficient is

$$D_{12} = \frac{\tilde{\alpha}}{\rho}\mu_x \tag{23}$$

the thermal diffusion coefficient is

$$D_T = \frac{T}{\rho}\left(\tilde{\alpha}\mu_T + \tilde{\beta}\right) \tag{24}$$

and the barodiffusivity is

$$D_P = \frac{\tilde{\alpha}P}{\rho}\left(\frac{\partial\mu}{\partial P}\right)_{T,x} \tag{25}$$

The thermodiffusion ratio, from Eqs. (6), (7) and (24), can be represented in the form

$$k_T = \frac{D_T}{D_{12}} = T\mu_T\mu_x^{-1}K(y) \tag{26}$$

with

$$K(y) = \frac{1+y^*}{1+y} \tag{27}$$

3. Regular parts of the transport coefficients

Eq. (6)–Eq. (8) for the kinetic coefficients in a binary mixture contain the shear viscosity and the regular (background) parts of the kinetic coefficients, as well as thermodynamic quantities. The viscosity η in these equations represents a shear viscosity which is an analytic function of temperature, density, and concentration. In the present work, unlike the previous works of Kiselev et al. [9–11], we use for the shear viscosity a simple corresponding-states correlation in the form

$$\eta(T,\rho,x) = \left[\frac{1-x}{\eta^{(1)}(T,\rho)} + \frac{x}{\eta^{(2)}(T,\rho)}\right]^{-1} \tag{28}$$

where the superscripts $i = 1,2$ denote the components of the mixture. As we will show below in the critical region at densities $0.35\rho_c \le \rho \le 1.65\rho_c$, where the crossover functions differ from zero, Eq. (28) in spite of its simplicity provides a good representation of the shear viscosity of binary mixtures.

There are no experimental data nor any adequate theoretical prediction for the dependencies of the kinetic coefficients $\tilde{\alpha}$, $\tilde{\beta}$ and $\tilde{\gamma}$ on temperature, density, and concentration far away from the critical point where these coefficients tend to their background parts $\tilde{\alpha}_b$, $\tilde{\beta}_b$ and $\tilde{\gamma}_b$, respectively. It is known only that even in the dilute gas limit the binary diffusion coefficient D, the thermal diffusion coefficient D_T and the thermal conductivity of a binary mixture are complex functions of the temperature, the concentration and molecular mass [25]. The primary concentration dependence of the coefficients $\tilde{\alpha}$ and $\tilde{\beta}$ in the dilute gas limit and in dilute solutions is given by $\sim x(1-x)$ [7,8]. In the present work, by analogy with the transport properties of one-component fluids [26,27] the background parts of the kinetic coefficients $\tilde{\alpha}$ and $\tilde{\beta}$ are given by

$$\tilde{\alpha}_b(T,\rho,x) = \tilde{\alpha}_0(T,x) + \tilde{\alpha}_{ex} \tag{29}$$

$$\tilde{\beta}_b(T,\rho,x) = \tilde{\beta}_0(T,x) + \tilde{\beta}_{ex} \tag{30}$$

where $\tilde{\alpha}_0(T,x)$ and $\tilde{\beta}_0(T,x)$ correspond to the dilute gas parts of the kinetic coefficients, and $\tilde{\alpha}_{ex}$ and $\tilde{\beta}_{ex}$ are the excess functions. In general, $\tilde{\alpha}_{ex}$ and $\tilde{\beta}_{ex}$ depend on the density, composition and temperature; however in the present work for simplicity we treated them as functions of the density and composition only, so that

$$\tilde{\alpha}_{ex}(\rho,x) = x(1-x)\frac{R^{-7/6}}{T_{ex}\Gamma_{ex}}\sum_{k=1}^{6}(\alpha_{3k} + \alpha_{3k+1}x)\left(\frac{\rho}{\rho_{cx}}\right)^{k+1} \tag{31}$$

$$\tilde{\beta}_{ex}(\rho,x) = x(1-x)\frac{R^{-1/6}}{T_{ex}\Gamma_{ex}}\sum_{k=1}^{6}(\beta_{3k} + \beta_{3k+1}x)\left(\frac{\rho}{\rho_{cx}}\right)^{k+1} \tag{32}$$

The form of Eq. (29)–Eq. (32) coincides with the form of corresponding equations employed earlier by Kiselev et al. [9–11] except that we introduce in Eqs. (31) and (32) the composition-dependent coefficient

$$\Gamma_{cx} = \frac{T_{cx}^{1/6} Z_{cx}^{5}\sqrt{M_{mix}}}{P_{cx}^{2/3}} \tag{33}$$

(where M_{mix} is the molecular mass of the mixture, T_{cx} and P_{cx} are the critical temperature and the

critical pressure of the mixture, and the critical compressibility factor $Z_{cx} = P_{cx}/R\rho_{cx}T_{cx}$), used earlier by Stiel and Thodos [28] in the corresponding states expression for the thermal conductivity of binary mixtures.

The background contribution of the kinetic coefficients $\tilde{\gamma}$ is given by

$$\tilde{\gamma}_b = \lambda_0(T,x) + \lambda_{ex}^{(1,2)} + T\frac{\tilde{\beta}_b^2(T,\rho,x)}{\tilde{\alpha}_b(T,\rho,x)} + x(1-x)\frac{R^{5/6}}{\Gamma_{cx}}\sum_{k=1}^{6}(\gamma_{2k-1} + \gamma_{2k}x)\left(\frac{\rho}{\rho_{cx}}\right)^k \tag{34}$$

In Eq. (29)–Eq. (34), $R = 8314.51$ J kmol^{-1} K^{-1} is the universal gas constant, P_{cx} is in MPa, T_{cx} is in K, $\tilde{\alpha}_b$ is in kg s m^{-3}, $\tilde{\beta}_b$ is in kg m^{-1} s^{-1} K^{-1}, $\tilde{\gamma}_b$ is in W m^{-1} K^{-1}, and α_k, β_k and γ_k ($k \geq 1$) are the system-dependent coefficients. The excess function $\lambda_{ex}^{(1,2)}$ is given by

$$\lambda_{ex}^{(1,2)} = \lambda_{ex}^{(1)}\frac{\left[T_c^{(1)}\right]^{1/6}\left[Z_c^{(1)}\right]^5\sqrt{M_1}}{\Gamma_{cx}\left[P_c^{(1)}\right]^{2/3}}(1-x) + \lambda_{ex}^{(2)}\frac{\left[T_c^{(2)}\right]^{1/6}\left[Z_c^{(2)}\right]^5\sqrt{M_2}}{\Gamma_{cx}\left[P_c^{(2)}\right]^{2/3}}x \tag{35}$$

where $\lambda_{ex}^{(1)}$ and $\lambda_{ex}^{(2)}$ define the excess parts of the thermal conductivity λ_b in the limits of the pure components, and the dilute gas parts of the kinetic coefficients are given by [9–11]

$$\tilde{\alpha}_0 = \frac{\rho D_0 M_{mix}^2}{RT}x(1-x) \tag{36}$$

$$\tilde{\beta}_0 = R\tilde{\alpha}_0\left(\beta_1 + x\beta_2 - \ln\frac{x}{1-x}\right) \tag{37}$$

$$\tilde{\gamma}_0(T,x) = \lambda_0(T,x) + T\frac{\tilde{\beta}_0^2(T,x)}{\tilde{\alpha}_0(T,x)} \tag{38}$$

For the binary diffusion coefficient in the dilute gas limit we use an empirical correlation proposed by Fuller and Giddings [29] and Fuller et al. [30]

$$D_0 = \frac{1.01325\times10^{-8}T^{1.75}\left[\frac{M_1+M_2}{M_1M_2}\right]^{\frac{1}{2}}}{P\left[\left(\sum v_1\right)^{\frac{1}{3}} + \left(\sum v_2\right)^{\frac{1}{3}}\right]^2} \tag{39}$$

(where T is in K, P in MPa, and D_0 in m^2 s^{-1}), and for the dilute gas part of the thermal conductivity $\lambda_0(T,x)$ we use a simple expression proposed by Wassilijeva [31]

$$\lambda_0(T,x) = \frac{(1-x)\lambda_0^{(1)}(T)}{(1-x)+xA_{12}} + \frac{x\lambda_0^{(2)}(T)}{x+(1-x)A_{21}} \tag{40}$$

with the Lindsay and Bromley [32] modification for A_{12} and A_{21}:

$$A_{12} = \frac{1}{4}\left\{1 + \left[\frac{\eta^{(1)}(T,0)}{\eta^{(2)}(T,0)}\left(\frac{M_2}{M_1}\right)^{\frac{3}{4}}\frac{T+S_1}{T+S_2}\right]^{\frac{1}{2}}\right\}^2 \frac{T+S_{12}}{T+S_1}$$

$$A_{21} = \frac{1}{4}\left\{1 + \left[\frac{\eta^{(2)}(T,0)}{\eta^{(1)}(T,0)}\left(\frac{M_1}{M_2}\right)^{\frac{3}{4}}\frac{T+S_2}{T+S_1}\right]^{\frac{1}{2}}\right\}^2 \frac{T+S_{12}}{T+S_2} \tag{41}$$

Here, $\lambda_0^{(i)}$ $(i = 1,2)$ is the thermal conductivity in the dilute gas limit, $S_1 = 1.5T_{nb}^{(1)}$, $S_2 = 1.5T_{nb}^{(2)}$ and $S_{12} = \sqrt{S_1 S_2}$ are Sutherland constants [32], and $T_{nb}^{(1)}$ $(i = 1,2)$ are the normal boiling temperatures of the pure components. To determine D_0 and λ_0 for the carbon dioxide + ethane and methane + ethane mixtures we use the following values of the atomic diffusion volumes and normal boiling temperatures [2] [33]

$$\Sigma v_{(CO_2)} = 26.90, \quad \Sigma v_{(CH_4)} = 24.42, \quad \Sigma v_{(C_2H_6)} = 44.88 \tag{42}$$

$$T_{nb}^{(CO_2)} = 194.7\,K, \quad T_{nb}^{(CH_4)} = 111.7\,K, \quad T_{nb}^{(C_2H_6)} = 184.5\,K \tag{43}$$

The correlation length $\hat{\xi}$ is given by Eq. (16), where for the bare correlation length ξ_0 and the cutoff parameter q_D in binary mixtures we use simple linear approximations

$$\xi_0 = \xi_0^{(1)}(1-x) + \xi_0^{(2)}x \tag{44}$$

$$\frac{1}{q_D} = \frac{1}{q_D^{(1)}}(1-x) + \frac{1}{q_D^{(2)}}x \tag{45}$$

where superscripts $i = 1,2$ denote the components of the mixture.

4. Transport coefficients of pure components

The background transport properties for methane, ethane and carbon dioxide are represented as sums of terms for the temperature dependent dilute gas contributions and terms for the temperature and density dependent excess contributions. Contributions for critical enhancement are not included in these background functions. High accuracy representations of the pure fluid background equations are available [34–37], however, we have chosen to illustrate the method with equations that can be used when the data is more limited and high accuracy correlations are not available. The viscosity is found using

$$\eta(\rho,T) = \eta_0(T) + \eta_{ex}(\rho,T) \tag{46}$$

while the thermal conductivity is given by

$$\lambda(\rho,T) = \lambda_0(T) + \lambda_{ex}(\rho,T) \tag{47}$$

[2] For CO_2, T_{nb} have been obtained by the extrapolation of the vapor–liquid saturation curve at the normal atmospheric pressure $P = 1$ atm.

Table 1
Lennard Jones potential parameters, ξ_0 and q_D^{-1} for pure fluids

Fluid	ϵ/k_B (K)	σ (nm)	ξ_0 (nm)	q_D^{-1} (nm)
Methane	148.6	0.3758	0.181	0.5554
Ethane	215.7	0.4443	0.190	0.5827
Carbon dioxide	195.2	0.3941	0.150	0.5056

The dilute gas viscosity is obtained from kinetic theory [38] assuming a Lennard–Jones potential applies and using the expression

$$\eta_0(T) = 26.69167 \times 10^{-9} \frac{\sqrt{MT}}{\Omega^{(2,2)}\sigma^2} \tag{48}$$

where η is in Pa s, M is the molecular mass, T is in K, $\Omega^{(2,2)}$ is a collision integral, and σ is the distance at which the potential energy function is zero, in nm. The collision integral for a Lennard Jones potential is evaluated using [39]

$$\Omega^{(2,2)}(t) = \frac{C_1}{t^{C_2}} + C_3 \exp(-C_4 t) + C_5 \exp(-C_6 t) \tag{49}$$

where $C_1 = 1.16145$, $C_2 = 0.14874$, $C_3 = 0.52487$, $C_4 = 0.77320$, $C_5 = 2.16178$ and $C_6 = 2.43787$, and $t = k_B T/\epsilon$. The potential energy parameters ϵ and σ were obtained from Ref. [33] and are listed in Table 1. The excess portion of the viscosity is found with an equation of the form found in [40]

$$\eta_{ex}(\rho,T) = 10^{-7} \exp\left(a_1 + \frac{a_2}{T}\right)\left(\exp\left[\left(a_3 + \frac{a_4}{T^{3/2}}\right)\rho^{0.1} + \left(\frac{\rho}{\rho_c} - 1\right)\rho^{1/2}\left(a_5 + \frac{a_6}{T} + \frac{a_7}{T^2}\right)\right] - 1\right) \tag{50}$$

where the excess viscosity is in Pa s, the temperature is in K, and the density is in mol l^{-1}. The coefficients for excess viscosity are from [41] and are given in Table 2. The dilute gas thermal conductivity is found from kinetic theory using a sum of rotational and transitional contributions

$$\lambda_0(T) = \left[f_1(T)\left[C_P^0(T) - \frac{5}{2}R\right] + \frac{15}{4}R\right]\frac{\eta_0(T) \times 10^{-6}}{M} \tag{51}$$

where λ_0 is in mW m^{-1} K^{-1}, C_p^0 is the ideal gas heat capacity in J mol^{-1} K^{-1}, and η_0 is in Pa s,

Table 2
Coefficients for excess viscosity

a_i	Methane	Ethane	Carbon dioxide
1	−11.1460	−9.83026	−2.88240
2	442.232	274.922	−2197.33
3	11.9729	12.0085	7.78198
4	−40,000.8	−3900.84	23,144.8
5	0.01285	0.05188	0.54518
6	13.2309	24.1829	−190.691
7	1873.14	2391.80	16,158.2

Table 3
Coefficients for ideal gas heat capacity

g_i	Methane	Ethane	Carbon dioxide
1	4.0	4.00644	3.50
2	3.00573	1.31139	2.00778
3	1870.00	465.008	960.11
4	1.82529	7.80610	0.97524
5	2180.00	1531.30	1932.0
6	4.07954	7.24643	1.08279
7	4170.00	3401.32	3380.2

while the function f_1 is given as

$$f_1 = 1.35558587 - 0.11306676\frac{T_c}{T} \tag{52}$$

The ideal gas heat capacities are written as

$$\frac{C_P^0(T)}{R} = g_1 + \sum_{j=1}^{3} g_{2j}\exp\left(\frac{g_{2j+1}}{T}\right)\frac{\frac{g_{2j+1}}{T}}{\exp\left(\frac{g_{2j+1}}{T}\right)-1} \tag{53}$$

The coefficients for ideal gas heat capacity are given in Table 3 [41]. The excess thermal conductivity function is a function of both temperature and density and is given by

$$\lambda_{ex}(\rho,T) = \frac{\rho}{\rho_c}\left[b_1 + b_2\left(\frac{\rho}{\rho_c}\right)^2 + \left(b_3 + b_4\frac{T_c}{T}\right)\left(\frac{\rho}{\rho_c}\right)^3 + \left(b_5 + b_6\frac{T_c}{T}\right)\left(\frac{\rho}{\rho_c}\right)^4\right] \tag{54}$$

where λ_{ex} is in mW m^{-1} K^{-1}. The excess thermal conductivity is a weak function of temperature, but a strong function of density. The coefficients for the excess thermal conductivity are given in Table 4 [41].

If the background transport properties of the pure components are known our crossover model contains two adjustable parameters: the bare correlation length $\xi_0^{(i)}$ and the cutoff parameter $q_D^{(i)}$. The parameter $\xi_0^{(i)}$ determines the critical amplitude of the correlation length in the asymptotic critical region and can be independently determined from light scattering measurements. For pure carbon dioxide, methane and ethane we adopt the same values for $\xi_0^{(i)}$ as used by Sengers and Olchowy [27] and Sengers and Levelt Sengers [42], while the parameters q_D^i are determined from a fit of the

Table 4
Coefficients for excess thermal conductivity

b_i	Methane	Ethane	Carbon dioxide
1	21.30511	16.4265	14.5845
2	11.07070	10.7440	20.9392
3	−5.744289	−6.13841	−14.0533
4	0.140431	0.33633	2.14884
5	1.670839	1.78933	3.75428
6	−0.095669	−0.19234	−0.98048

crossover Eq. (19) to experimental thermal conductivity data in the critical region [43–45]. The parameters $\xi_0^{(i)}$ and q_D^i for carbon dioxide, methane and ethane are presented in Table 1. The thermal conductivity for carbon dioxide, methane and ethane in the critical region are plotted in Figs. 1–3. Percentage deviations of the experimental thermal conductivity from the calculated values beyond the critical region are shown in Figs. 4–6. Since the crossover equations of state used for the calculation of all thermodynamic quantities for carbon dioxide [11], methane and ethane [16] do not reproduce the ideal gas limit at low densities, and may even give unphysical behavior as $\rho \to 0$, we restrict our calculations to the fluid regions

$$\rho \geq \left[0.25 + 0.15(T/T_c - 1)^2\right] \rho_c \tag{55}$$

for carbon dioxide, and

$$\rho \geq 0.25\rho_c \tag{56}$$

for methane and ethane. The percentage deviations of the thermal conductivity are less than 4% over the entire thermodynamic surface for densities specified by Eqs. (55) and (56) and increase up to 8–10% at the boundary.

5. Transport properties of binary mixtures

In order to apply our crossover model to the calculation of the transport properties in binary mixtures, in addition to the equation of state and expressions for the background transport coefficients for pure components $\lambda_b^{(i)}(T, \rho)$ and $\eta_b^{(i)}(T, \rho)$, one needs also the coefficients α_k, β_k and γ_k in Eqs. (29) and (34) for the background coefficients $\tilde{\alpha}_b$, $\tilde{\beta}_b$ and $\tilde{\gamma}_b$. The background coefficients $\tilde{\alpha}_b$ and $\tilde{\beta}_b$ not only determine the crossover behavior of the thermal conductivity of a binary mixture in the critical region as given by Eq. (19)–Eq. (21), but also determine the binary diffusion coefficient D

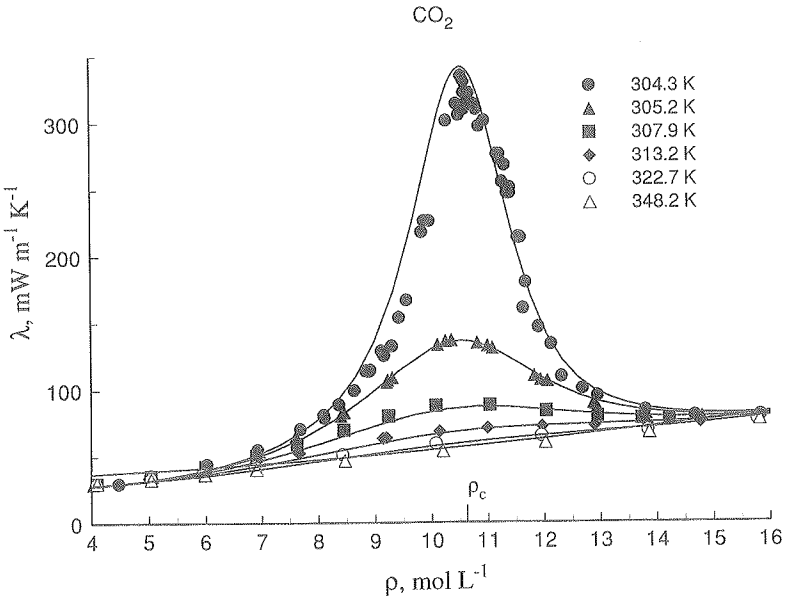

Fig. 1. The thermal conductivity of carbon dioxide as a function of the density along isotherms. The symbols indicate experimental data obtained by Michels et al. [43], and the curves represent values calculated with the crossover model.

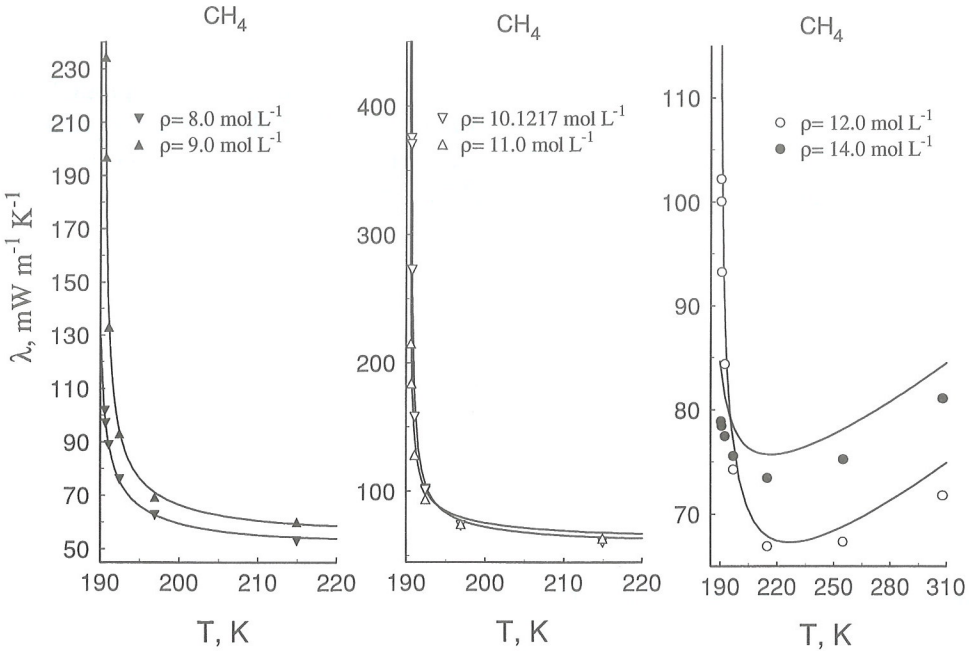

Fig. 2. The thermal conductivity of methane as a function of the temperature along isochores. The symbols indicate experimental data obtained by Sakonidou [44], and the curves represent values calculated with the crossover model.

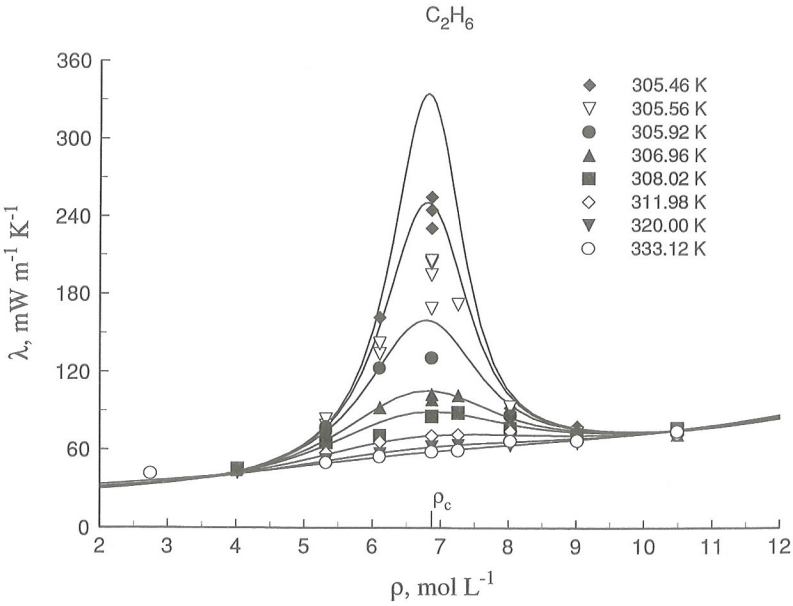

Fig. 3. The thermal conductivity of ethane as a function of the density along isotherms. The symbols indicate experimental data obtained by Mostert [46], and the curves represent values calculated with the crossover model.

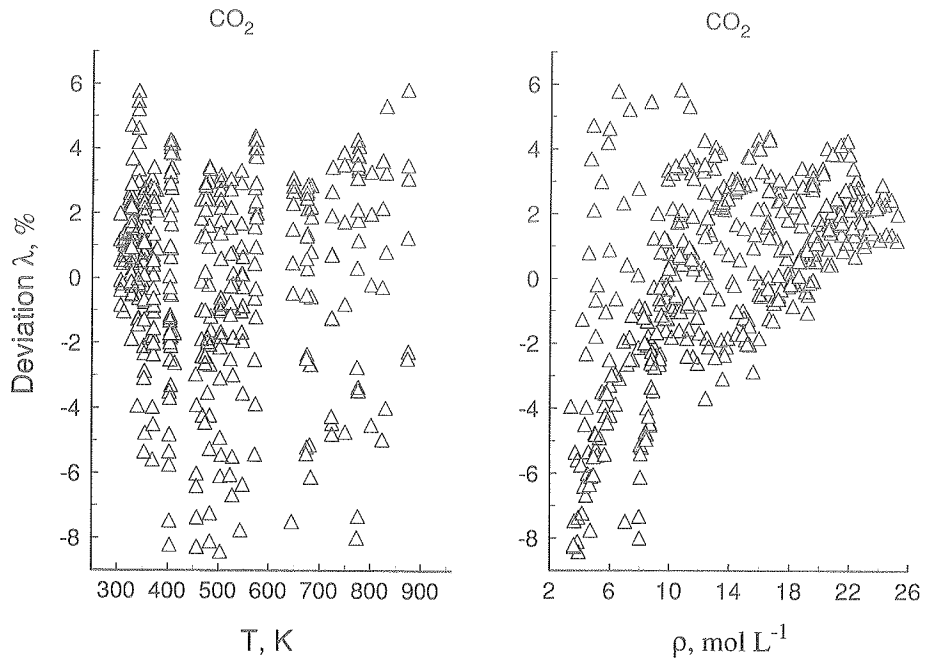

Fig. 4. Percentage deviations of experimental thermal conductivity for carbon dioxide of Le Niendre et al. [47,48] from values calculated with the crossover model.

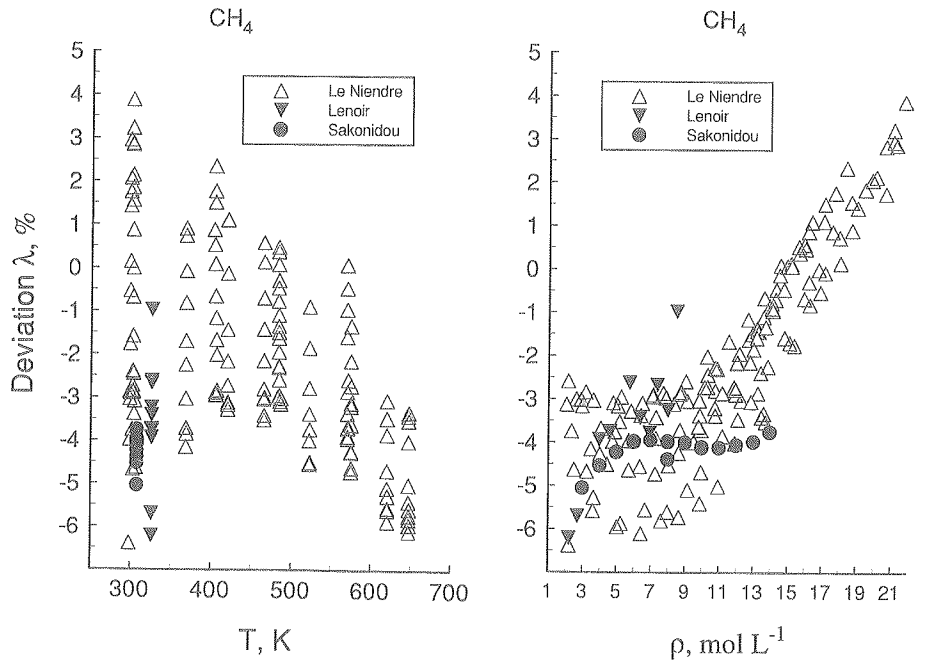

Fig. 5. Percentage deviations of experimental thermal conductivity for methane of Le Niendre et al. [49], of Lenoir et al. [50], and of Sakonidou [44] from values calculated with the crossover model.

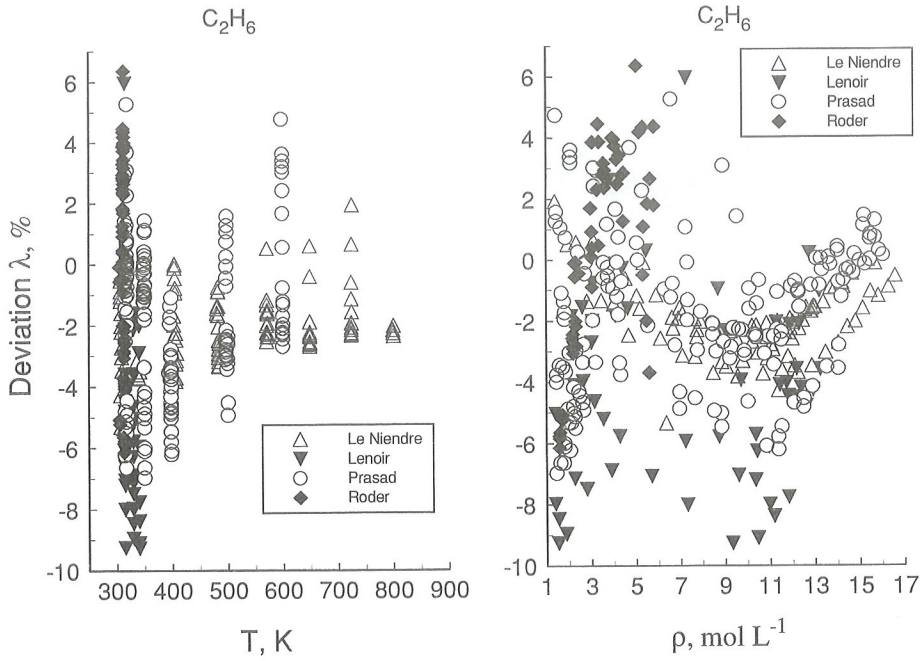

Fig. 6. Percentage deviations of experimental thermal conductivity for ethane of Le Niendre et al. [49,47], of Lenoir et al. [50], of Prasad and Venart [51], and of Roder [52] from values calculated with the crossover model.

and the thermal diffusion coefficient D_T of binary mixtures far away from the critical point (see Eqs. (23) and (24)). We do not have experimental binary diffusion coefficient data for carbon dioxide + ethane and methane + ethane mixtures, therefore, we found the coefficients α_k from fitting the crossover Eq. (6) together with Eqs. (23) and (29) to binary diffusion coefficient data generated with an empirical correlation for binary fluid mixtures [53]

$$D\eta = \left(D_{12}^0 \eta^{(2)}\right)^{x_2} \left(D_{21}^0 \eta^{(1)}\right)^{x_1} \tag{57}$$

where x_1 and x_2 are the molar fractions of the components, and the dilute-solution binary diffusion coefficients D_{12}^0 and D_{21}^0 are calculated with an empirical modification of the Stokes–Einstein equation for the diffusion coefficient [54]

$$D_{ij}^0 = \frac{8.52\,10^{-15} T}{\eta^{(j)} V_j^{\frac{1}{3}}} \left[1.40 + \left(\frac{V_j}{V_i}\right)^{\frac{2}{3}}\right] \tag{58}$$

Here T is in K, η in Pa s, D_{ij}^0 in $m^2\ s^{-1}$, V_j and V_i in $cm^3\ mol^{-1}$ are the molar volumes of components at their normal boiling temperatures. Here, we use [3] [33]

$$V_{CO_2} = 55.024,\ V_{CH_4} = 37.936,\ V_{C_2H_6} = 37.321 \tag{59}$$

[3] For CO_2, we use the molar volume of liquid carbon dioxide at the triple point.

5.1. Carbon dioxide + ethane mixture

The coefficients β_k for carbon dioxide + ethane mixtures have been found from fitting of Eqs. (7) and (26), at fixed values of the coefficients α_k (the α_k were found using binary diffusion coefficient data as described in the previous paragraph), to the experimental thermal diffusion ratio data obtained by Walther [55]. The thermodynamic properties for carbon dioxide and ethane mixtures were calculated from the new crossover equation of state obtained recently by Kiselev and Kulikov [11]. The results of comparison with thermal diffusion ratio data for the carbon dioxide and ethane mixture is shown in Fig. 7. Good agreement between calculated values and experimental data of Walther [55] for the thermal diffusion ratio is observed. As one can see from Fig. 7, the thermal diffusion ratio increases in the critical region and reaches a maximum at a density close to the critical density. Along the critical isotherm (which corresponds to the temperature $T = 290.854$ K at this composition), the thermal diffusion ratio diverges as $\rho \to \rho_c$.

The coefficients γ_k in Eq. (34) for carbon dioxide and ethane mixtures have been found from a fit of the crossover Eq. (19) (with the found above values of the coefficients α_k and β_k), to the experimental thermal conductivity data in the critical region obtained by Mostert [46]. Since the actual composition at which the thermal conductivity was measured differed from that of the sample upon filling, as discussed by Luettmer-Strathmann and Sengers [15], we excluded from the calculations thermal conductivity data apparently corresponding to the two-phase region and, as in our previous work [11], shifted the temperatures associated with the thermal conductivity data of Mostert [46] by $\Delta T = +0.260$ K at $x = 0.26$, $\Delta T = -0.478$ K at $x = 0.50$, $\Delta T = -0.445$ K at $x = 0.74$, and $\Delta T = -0.463$ K at $x = 0.75$. The coefficients α_k, β_k and γ_k for carbon dioxide and ethane mixtures are presented in Table 5. Experimental and calculated thermal conductivity values for carbon dioxide

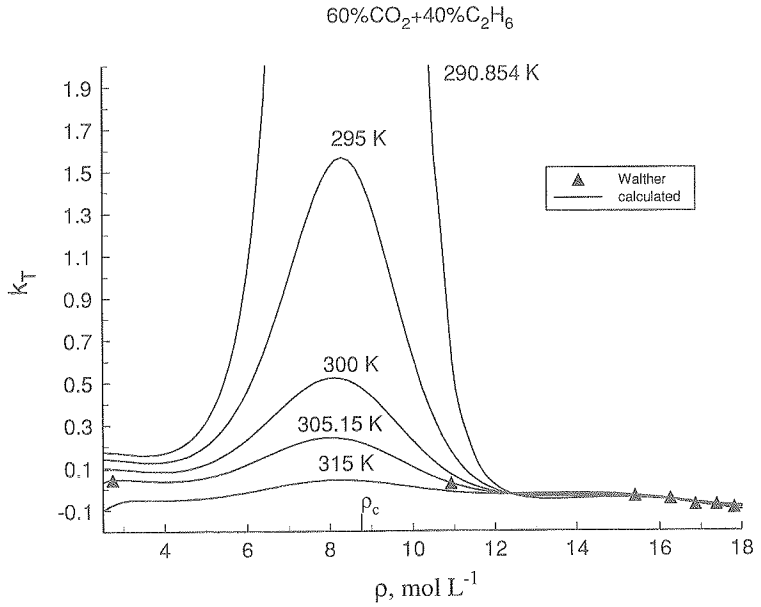

Fig. 7. The thermal diffusion ratio of the carbon dioxide and ethane mixture at the concentration $x = 0.4$ mole fraction of ethane along isotherms as a function of the density. The symbols indicate experimental data obtained by Walther [55] at the temperature $T = 305.15$ K and the curves represent values calculated with the crossover model.

Table 5
The background kinetic coefficients α_k, β_k, and γ_k used in Eqs. (31), (32) and (34) for carbon dioxide + ethane mixture

Coefficients $\tilde{\alpha}_b$		Coefficients $\tilde{\beta}_b$		Coefficients $\tilde{\gamma}_b$	
α_6	1.33315×10^{-6}	β_1	2.40238	γ_1	-1.17562×10^{-6}
α_7	-2.34664×10^{-6}	β_3	-7.43324×10^{-6}	γ_2	-5.14420×10^{-7}
α_{12}	-1.43428×10^{-6}	β_6	6.39961×10^{-6}	γ_3	5.54845×10^{-6}
α_{13}	$1.70776\times\times10^{-6}$	β_{12}	-1.15818×10^{-6}	γ_5	-6.72675×10^{-6}
α_{18}	1.96473×10^{-7}	β_{18}	9.40929×10^{-8}	γ_6	2.60059×10^{-6}
α_{19}	-2.44598×10^{-7}			γ_9	1.74581×10^{-6}
				γ_{10}	-1.24763×10^{-6}

and ethane mixtures at various concentrations and densities are plotted as a function of temperature in Fig. 8. Good agreement between experimental data and calculated values is observed.

Another crossover equation for the thermal conductivity for carbon dioxide and ethane mixtures has recently been proposed by Kiselev and Kulikov [11]. Our crossover model differs from the corresponding crossover equations used earlier by Kiselev et al. [9–11] in two aspects. Firstly, we have used the renormalized correlation length Eq. (16), instead of the asymptotic expression employed by Kiselev et al. [9–11]. With this renormalization, all crossover functions tend to zero far away from the critical point, and the crossover equations in the critical region are not changed. Secondly, we have used here the modified expressions for the the shear viscosity and the kinetic

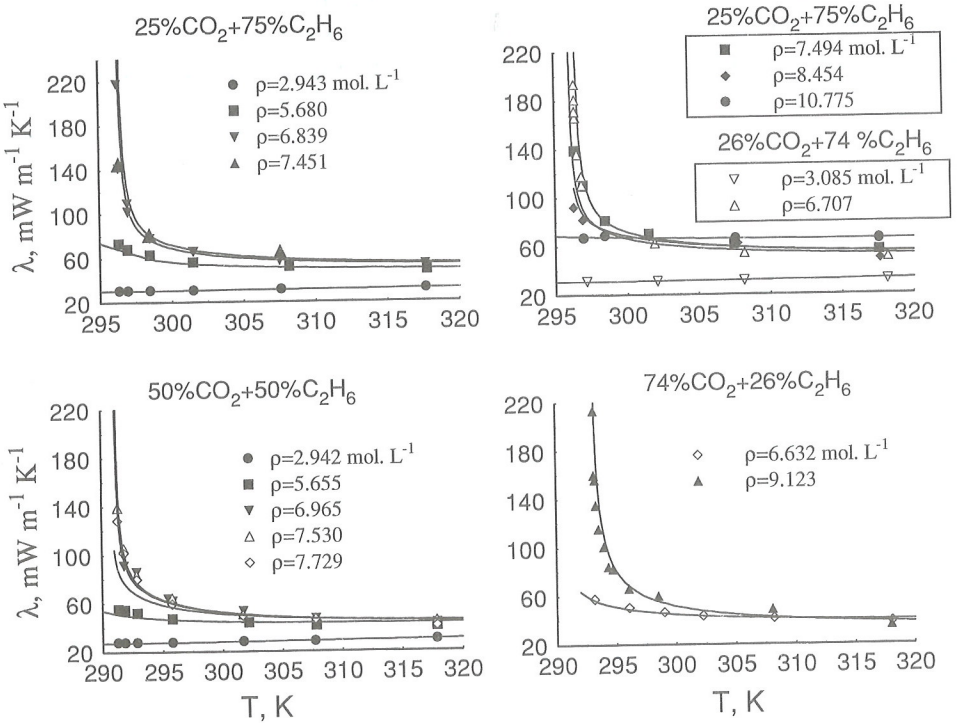

Fig. 8. The thermal conductivity of the carbon dioxide and ethane mixture at various compositions as a function of the temperature. The symbols indicate experimental data obtained by Mostert [46] and the curves represent values calculated with the crossover model.

coefficients $\tilde{\alpha}_b$, $\tilde{\beta}_b$, and $\tilde{\gamma}_b$ (see Eqs. (28), (31), (32) and (34). With the renormalization of the correlation length as given by Eq. (16) and with improved equations for the shear viscosity and the kinetic coefficients $\tilde{\alpha}_b$, $\tilde{\beta}_b$, and $\tilde{\gamma}_b$, the crossover model gives better representation of the thermal conductivity of non-critical isochores far away from the critical point than the earlier equation of Kiselev and Kulikov [11]. In the critical region, both equations yield essentially identical results.

It is also interesting to compare the result of our calculations for carbon dioxide and ethane mixtures with the results obtained by Luettmer-Strathmann and Sengers [15]. Quantitatively our calculations for the thermal conductivity in carbon dioxide and ethane mixtures and the mode-coupling calculations by Luettmer-Strathmann and Sengers [15] reproduce the experimental thermal conductivity data with similar accuracy. However, unlike the calculations of Luettmer-Strathmann and Sengers [15] which represents a fit of their crossover equations to experimental thermal conductivity data at separate compositions and isochores only, our crossover model can be used for the calculation

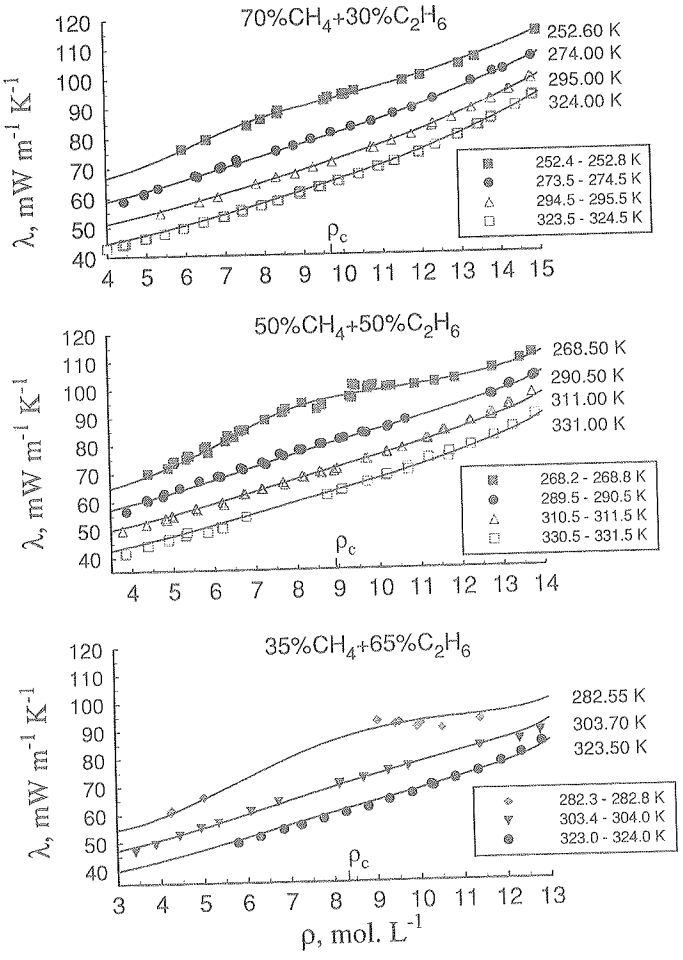

Fig. 9. The thermal conductivity of the methane and ethane mixture at various compositions as a function of the density. The symbols indicate experimental data obtained by Roder and Friend [56] and the curves represent values calculated with the crossover model, individual isotherms separated by 10 mW m^{-1} K^{-1}.

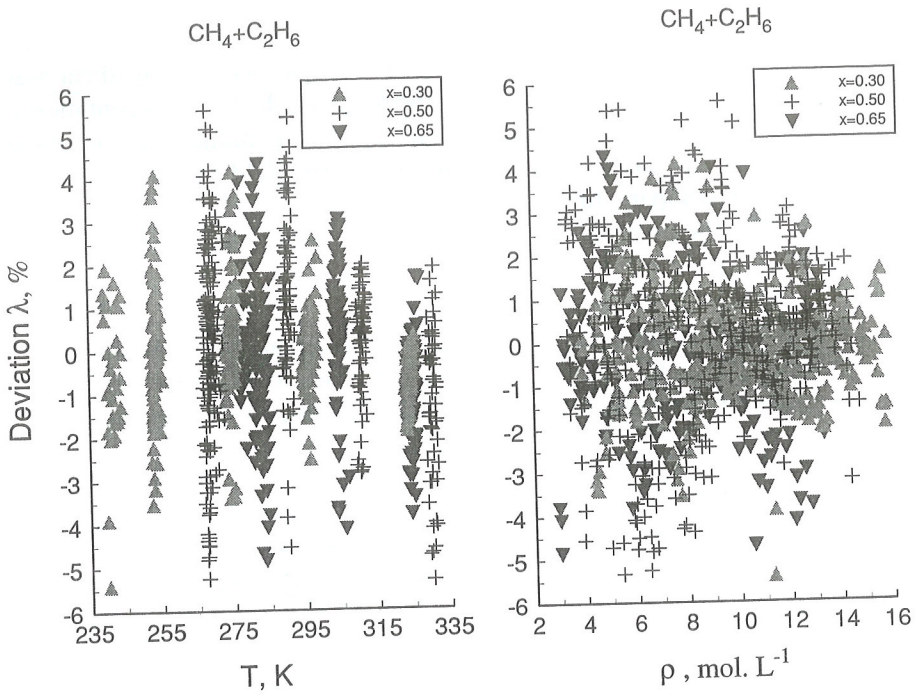

Fig. 10. Percentage deviations of experimental thermal conductivity for methane and ethane mixtures of Roder and Friend [56] from values calculated with the crossover model at various concentrations of ethane.

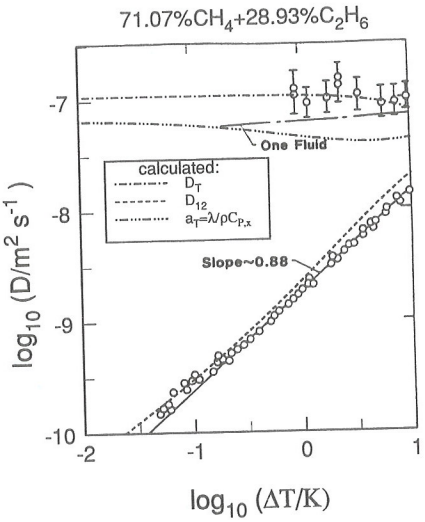

Fig. 11. The thermal- and binary-diffusion coefficients of the methane and ethane mixture as a function of temperature along the critical isochore at the concentration $x = 0.2893$ mole fraction of ethane. The symbols indicate experimental data obtained by Ackerson and Hanley [59], dashed and dotted–dashed curves represent the values calculated with the crossover model. The long-dashed curve corresponds to the one-fluid approximation and the solid curve corresponds to a fit to an exponential as discussed in Ref. [59].

Table 6
The background kinetic coefficients α_k, β_k and γ_k used in Eqs. (31), (32) and (34) for methane + ethane mixture

Coefficients $\tilde{\alpha}_b$		Coefficients $\tilde{\beta}_b$		Coefficients $\tilde{\gamma}_b$	
α_6	2.63729×10^{-6}	β_1	$-4.25925\times10^{+1}$	γ_1	2.14578×10^{-6}
α_7	-4.36365×10^{-6}	β_2	$1.33671\times10^{+2}$	γ_2	-6.78429×10^{-6}
α_{12}	-1.66614×10^{-6}	β_3	1.68885×10^{-4}	γ_3	-8.44631×10^{-6}
α_{13}	8.95098×10^{-7}	β_6	-1.70441×10^{-4}	γ_4	2.97397×10^{-5}
α_{18}	1.98466×10^{-7}	β_{12}	5.26569×10^{-5}	γ_5	1.35214×10^{-5}
		β_{18}	-8.18222×10^{-6}	γ_6	-4.48729×10^{-5}
		β_4	-4.83899×10^{-4}	γ_7	-8.51939×10^{-6}
		β_7	4.46871×10^{-4}	γ_8	2.77889×10^{-5}
		β_{13}	-1.16963×10^{-4}	γ_9	1.92812×10^{-6}
		β_{19}	1.51993×10^{-5}	γ_{10}	-6.19831×10^{-6}

of the transport properties of carbon dioxide and ethane mixtures over the entire thermodynamic surface from $x=0$ to $x=1$ in the range of temperatures and densities bounded by

$$\left(\frac{T}{T_{cx}}-1\right)+1.2\left(\frac{\rho}{\rho_{cx}}-1\right)^2\le 0.5;\ T\ge T_s(\rho,x) \tag{60}$$

where $T_s(\rho,x)$ is a saturated dew–bubble curve temperature at a given ρ and x. This range corresponds to the range of temperatures and densities where a good description of the thermody-

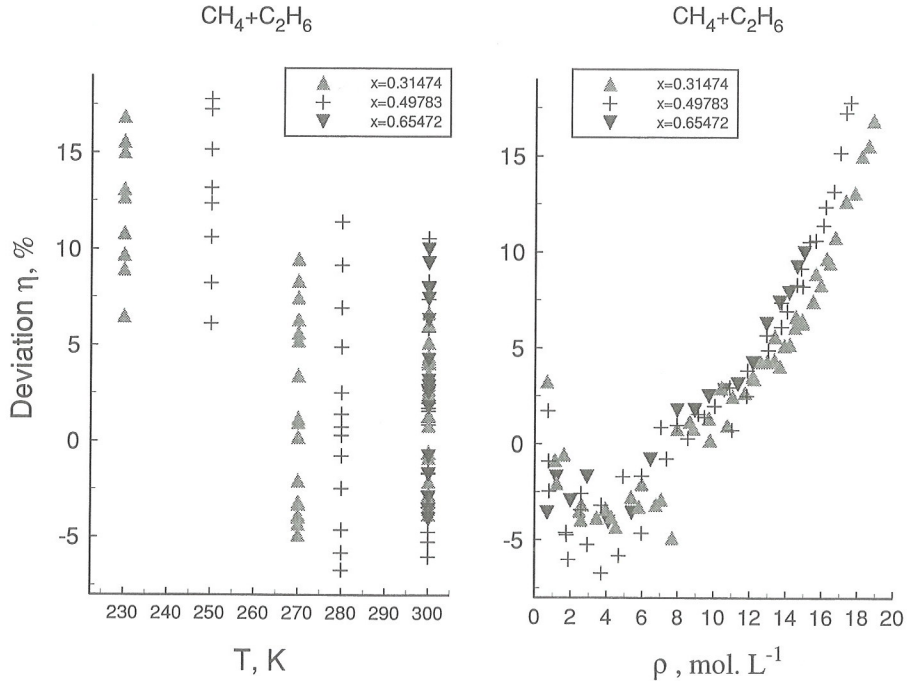

Fig. 12. Percentage deviations of experimental viscosity for methane and ethane mixtures of Diller [61] from values calculated with Eq. (28) at various concentrations of ethane.

namic properties of binary mixtures was achieved with the crossover equation of state used for the calculation of the thermodynamic derivatives in Eq. (19)–Eq. (21).

5.2. Methane + ethane mixture

Unlike the carbon dioxide and ethane mixture, for the methane and ethane mixtures we do not have experimental thermal diffusion ratio data far away from the critical region. Therefore, we found the coefficients β_k and γ_k from a fit of our model to the thermal conductivity data obtained by Roder and Friend [56] at three compositions of ethane. The thermodynamic properties for the methane and ethane mixtures were calculated from the new crossover equation of state obtained recently by Kiselev [16] as modified later by Kiselev and Rainwater [17]. The thermal conductivity for methane + ethane mixtures at various temperatures is plotted as a function of density in Fig. 9. Percentage deviations of the experimental thermal conductivity from the calculated values for methane and ethane mixtures are shown in Fig. 10. The percentage deviations are less than 3% inside the region specified by Eq. (60) and increase up to 4–5% at the boundary and in the critical region. These thermal conductivity deviations correspond approximately to those found by Roder and Friend [57,58]. However, in contrast to Refs. [57,58], our crossover model not only reproduces the thermal conductivity surface within experimental accuracy but also allows the prediction of the binary and thermal diffusion coefficients in a wide region around the critical locus. A comparison of calculated

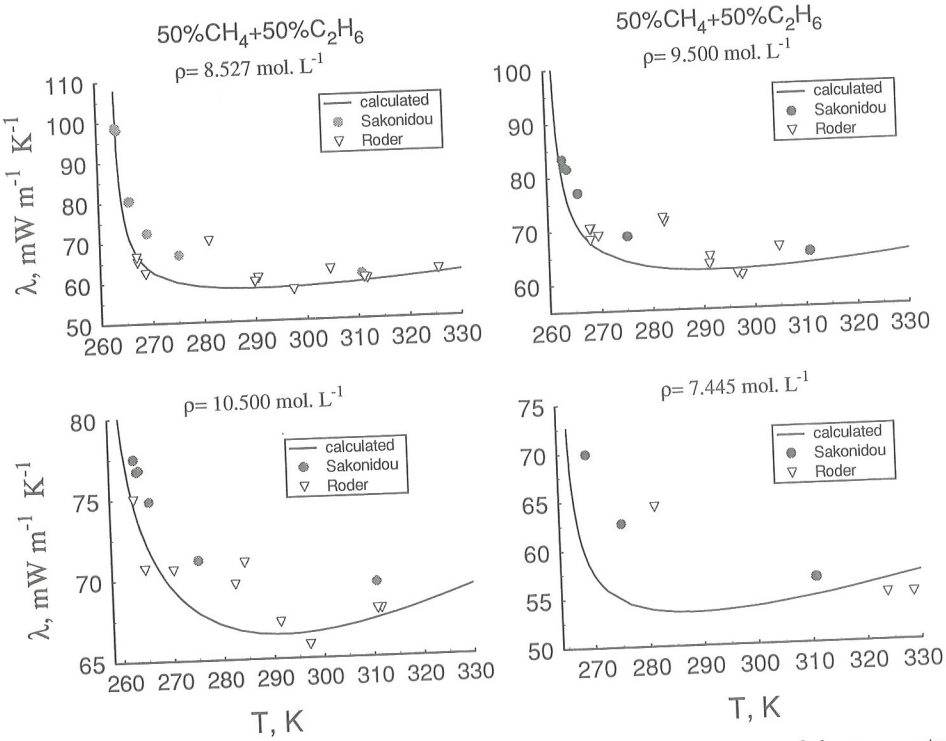

Fig. 13. The thermal conductivity of the 50% methane + 50% ethane mixture as a function of the temperature. The circles indicate experimental data obtained by Sakonidou [44], the triangles correspond to the experimental data of Roder and Friend [56], and the curves represent values calculated with the crossover model.

binary and thermal diffusion coefficients in the critical region of a 71.07% CH_4 + 28.93% C_2H_6 mixture with light scattering experimental data obtained by Ackerson and Hanley [59] is shown in Fig. 11. As one can see from Fig. 11 the calculated values of the binary diffusion coefficient lie slightly higher than experimental data. This small shift between the calculated values of the binary diffusion coefficient and light scattering data obtained by Ackerson and Hanley [59] can be removed with a corresponding shift of the background coefficient $\tilde{\alpha}_b$, which determines the binary diffusion coefficient of a mixture far away from the critical point (see Eq. (23)). However, as it was shown by Anisimov et al. [60], because of a coupling between two hydrodynamic modes the 'effective' binary diffusion coefficient associated with the light scattering experiment can lie lower than a 'pure' diffusion coefficient of a binary mixture. Since we do not have experimental binary diffusion coefficient data for methane and ethane mixtures far away from the critical point in the present paper we calculated the background coefficient $\tilde{\alpha}_0(T, x)$ with the coefficients α_k found above from a fit of Eqs. (36) and (39) to the data generated with Eq. (57). The coefficients α_k, β_k and γ_k for methane and ethane mixtures are listed in Table 6. All other coefficients which are not listed in this table equal zero.

Description of the shear viscosity of binary mixtures was not the aim of the present paper. The viscosity appears in the crossover functions Ω_α and Ω only in the definition of the dimensionless coefficients y_D and y_{1D} (see Eq. (11)–Eq. (14)). Since these coefficients also contain the background

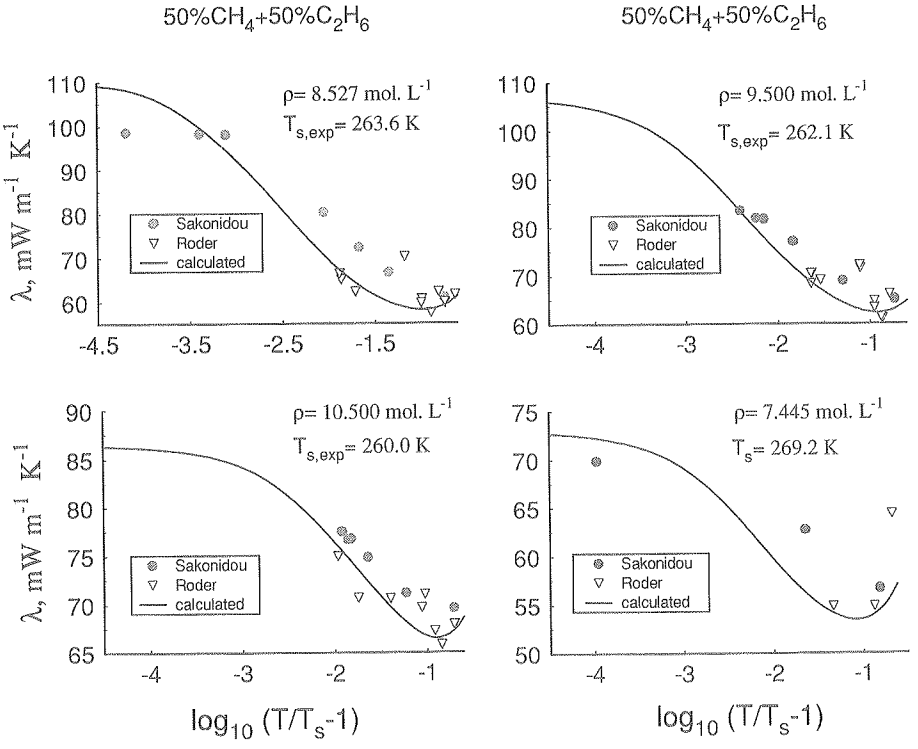

Fig. 14. The thermal conductivity of the 50% methane + 50% ethane mixture as a function of the dimensionless deviation of the temperature from the saturated dew–bubble curve temperature $T_s(\rho)$. The symbols indicate experimental data obtained by Sakonidou [44] (circles) and by Roder and Friend [56] (triangles), and the curves represent values calculated with the crossover model.

parts $\tilde{\alpha}_b$ and $\tilde{\gamma}_b$, and a cutoff wave number q_D (which are treated here as adjustable parameters), an accurate representation of the shear viscosity of a binary mixture is not crucial for our crossover model. However, it is interesting to note that even the simple corresponding-state relation (28) used in this work reproduces experimental shear-viscosity data in binary mixtures with reasonable accuracy. A comparison of the calculated viscosity for the methane + ethane mixtures with experimental data obtained by Diller [61] is shown in Fig. 12. The percentage deviations of the experimental viscosity from the calculated values are less than 5% inside the region specified by Eq. (60) (3 mol $l^{-1} \leq \rho \leq 15$ mol l^{-1}) and increase up to 15–20% at the high densities $\rho \geq 16$ mol l^{-1} ($\rho \geq 2\rho_c$), where all crossover functions tend to zero.

It is interesting also to compare our crossover model with the new experimental thermal conductivity data for the methane + ethane mixture obtained recently by Sakonidou [44] in the critical region. The thermal conductivity values for 50% methane + 50% ethane mixtures at various densities are plotted as a function of temperature in Fig. 13. A comparison of our calculations with the experimental thermal conductivity data along four isochores in the logarithmic temperature scale is

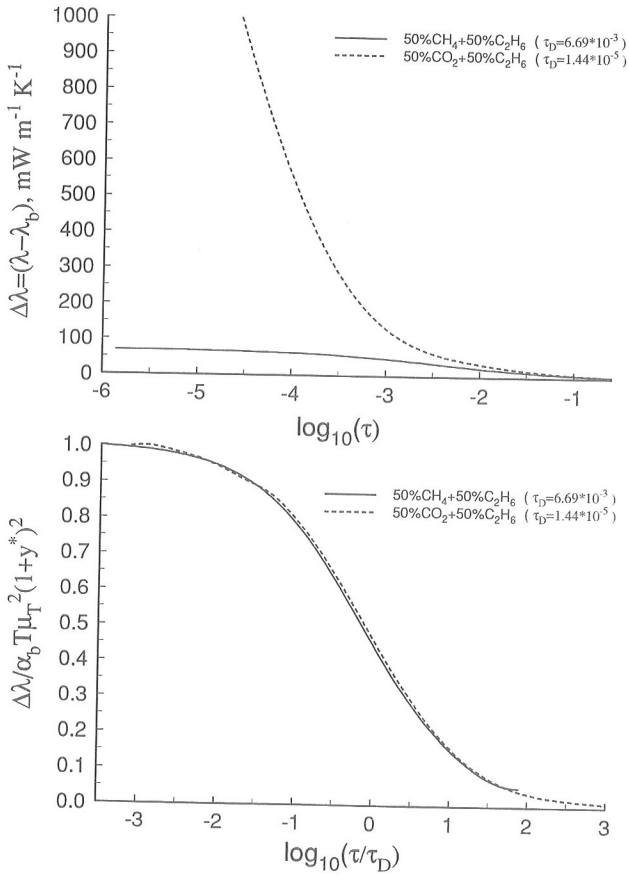

Fig. 15. The thermal conductivity of the 50% carbon dioxide + 50% ethane (dashed curve) and 50% methane + 50% ethane (solid curve) mixtures calculated with the crossover model as a function of the dimensionless temperature τ (top) and of the rescaled temperature $\tau = \tau/\tau_D$ (bottom) along the critical isochore.

shown in Fig. 13. Some scatter observed for the thermal conductivity data of Roder and Friend [56] in Figs. 13 and 14 is due to the fact that these data were obtained along the isotherms rather than isochores and the density of the experimental points does not exactly correspond to the nominal isochore density. Since the critical density calculated from the equation of state of Kiselev [16] for 50% methane + 50% ethane mixture is higher than that of Povodyrev et al. [62] (which Sakonidou [44] used as the critical density), we represent the calculated and the experimental thermal conductivity as a function of the dimensionless deviation of the temperature from the saturated dew–bubble curve temperature $T_s(\rho)$, but not T_c. The experimental values of the saturated temperature obtained by Sakonidou [44] differ from those calculated with the crossover equation of state [16], therefore, for the experimental data in Fig. 15 we used the experimental values of $T_s(\rho)$ obtained in Ref. [44]. There is not an exact experimental value of the saturated dew–bubble curve temperature at $\rho = 7.445$ mol l^{-1}, therefore we have chosen the value $T_s = 269.2 \pm 0.02$ K which corresponds to the lowest experimental temperature at this isochore. Our crossover model reproduces the experimental thermal conductivity data of Sakonidou [44] for methane and ethane mixtures with an accuracy comparable with the accuracy achieved for the thermal conductivity of pure methane and ethane in the critical region (see Figs. 2 and 3).

6. Discussion

The thermodynamic and transport properties of fluids and fluid mixtures exhibit singular behavior near the critical point and approach their regular background parts far away from the critical point. In order to describe the transport properties of binary mixtures in and beyond the critical region, in this paper we used the crossover model developed by Kiselev and Kulikov [8,11]. With this model we calculate the thermal conductivity for pure carbon dioxide, methane, ethane, and for the carbon dioxide + ethane and methane + ethane mixtures. Good agreement between experimental data and our model was achieved for binary mixtures inside the region specified by Eq. (60). This region is restricted not by the transport property crossover model of Kiselev and Kulikov [8,11], but by the accuracy of the crossover equation of state used for calculating the thermodynamic quantities which appear in the crossover equations for the transport coefficients. For pure fluids, good agreement between experimental and calculated thermal conductivity is observed over the entire thermodynamic surface for densities specified by Eq. (55) for carbon dioxide, and Eq. (56) for methane and ethane.

Our calculations are fully consistent with the results of the theoretical analysis performed earlier by Onuki [6] and by Kiselev et al. [7,8,11]. According to this analysis, the crossover behavior of the transport coefficients of a binary mixture along the critical isochore is determined by the characteristic temperature

$$\tau_D(x) \simeq \left[\frac{\rho_c \Gamma_0}{6\pi\eta(\rho_c, T_c)\xi_0 \tilde{\alpha}_b(\rho_c, T_c)} \right]^{\frac{1}{\gamma-\nu}} \tag{61}$$

In the temperature range $\tau_D \ll \tau$ (where $\tau = T/T_c - 1$) the thermal conductivity of a binary mixture behaves as the thermal conductivity of a pure fluid. Asymptotically close to the critical point at

$\tau \ll \tau_D$ the thermal conductivity of a binary mixture is renormalized and, unlike the thermal conductivity of a pure fluid, does not diverge and tends to a finite value at the critical point [8,11],[64]

$$\lim_{\tau(x)\to 0} \lambda = \lambda_{cb} = \lambda_b + T\mu_T^2 \tilde{\alpha}_b (1 + y^*)^2 \tag{62}$$

where the background part

$$\lambda_b = \tilde{\gamma}_b - T\frac{\tilde{\beta}_b^2}{\tilde{\alpha}_b} = \tilde{\gamma}_b - \tilde{\alpha}_b T\mu_T^2 (y^*)^2 \tag{63}$$

is not equal to the background contribution of the kinetic coefficient $\tilde{\gamma}$ given by Eq. (34) For the methane and ethane mixtures the renormalization of the thermal conductivity at temperatures $\tau \leq 10^{-3}$ was predicted earlier by Kiselev and Kulikov (see Fig. 5 in Ref. [8]). Our estimates for the characteristic temperature τ_D with Eq. (61) give for the 50% CO_2 + 50% C_2H_6 mixture $\tau_D = 1.44 \times 10^{-5}$, and $\tau_D = 6.69 \times 10^{-3}$ for the 50% CH_4 + 50% C_2H_6 mixture, that approximately correspond to the earlier results of Kiselev and Kulikov [8,11]. Calculated thermal conductivity at the critical isochore for the 50–50% carbon dioxide + ethane and methane + ethane mixtures as a function of the temperature is shown in Fig. 14. The results of our calculations confirm this theoretical prediction. One can see that the calculated curves for carbon dioxide + ethane and for methane + ethane mixtures appear to be quite different functions of the dimensionless temperature τ. However, the dimensionless singular part of the thermal conductivity $\Delta\bar{\lambda} = \Delta\lambda/\tilde{\alpha}_b T\mu_T^2(1 + y^*)^2$ is a universal function of the rescaled temperature $\bar{\tau} = \tau/\tau_D$. Far away from the critical point $\Delta\bar{\lambda} \to 0$, at temperatures $\tau_D \ll \tau < 1$ the singular part $\Delta\bar{\lambda}$ increases as in a pure fluid, and at temperatures $\tau \simeq \tau_D$ the thermal conductivity of both binary mixtures exhibits the crossover from the one-component like behavior to the critical background as given by Eq. (62).

Qualitatively this result agrees with the experimental data and the direct mode-coupling calculations of Sakonidou et al. [44,63]. However, the critical background value obtained in the present paper for the methane + ethane mixture is about 15% larger than that in Ref. [44,63]. At the isochore $\rho = 8.527$ mol l^{-1}, accepted by Sakonidou et al. [44,63] as the critical isochore, the difference is about 5–6%. According to the theoretical prediction [8,11] the critical background value of the thermal conductivity in a binary mixture is mostly determined by the values of the background parts of the kinetic coefficients $\tilde{\alpha}$ and $\tilde{\beta}$ at the critical point. Our estimates with Eq. (29)–Eq. (32) at the critical temperature and density for the 50% methane + 50% ethane mixture give $\tilde{\alpha}_b = 3.506 \times 10^{-11}$ kg s m^{-3} and $\tilde{\beta}_b = -1.94 \times 10^{-8}$ kg m^{-1} s^{-1} K^{-1}, which substantially differ from those of Sakonidou et al. [44,63]: $\tilde{\alpha}_b = 7.086 \times 10^{-12}$ kg s m^{-3} and $\tilde{\beta}_b = 6.35 \times 10^{-9}$ kg m^{-1} s^{-1} K^{-1}. Sakonidou et al. [44,63] found the background contributions $\tilde{\alpha}_b$ and $\tilde{\beta}_b$ from a fit of the mode-coupling crossover model [15] to their own experimental thermal conductivity data obtained by the parallel plate method which is more reliable for measuring the thermal conductivity in the critical region than the hot wire method used by Roder and Friend [56]. However, the experimental data of Sakonidou et al. [44,63] is restricted to the near vicinity of the critical point in the 50% methane + 50% ethane mixture, where the evident discrepancy between two data sets is observed; therefore, we can not use them in a simultaneous fit with the Roder and Friend data [56]. Moreover, since the background coefficients $\tilde{\alpha}_b$ and $\tilde{\beta}_b$ not only influence the crossover behavior of the thermal conductivity of a binary mixture in the critical region, but also determine the thermal-and binary-diffusion coefficients far away from the critical region (see Eqs. (23) and (24)), it is important to have

more experimental data for thermal and binary diffusion coefficients in methane + ethane mixtures so that better values of $\tilde{\alpha}_b$ and $\tilde{\beta}_b$ may be found.

7. List of symbols

a_i	Coefficient of excess viscosity
A_{12}	Coefficient of dilute gas thermal conductivity
b_i	Coefficient of excess thermal conductivity
C_i	Coefficients of collision integral
C_P	Isobaric heat capacity
D	Diffusion coefficient
f_λ	Coefficient of dilute gas thermal conductivity
$\vec{J}_d$	Diffusion current
$\vec{J}_q$	Heat current
g_i	Coefficient of ideal gas heat capacity
K	Crossover function
k_B	Boltzmann's constant
k_T	Thermodiffusion ratio
M	Molecular mass
P	Pressure
Q	Crossover function
q_D	Cutoff wave number
R	Gas constant
S	Molar entropy
S_{12}	Sutherland constant
T	Temperature
t	Dimensionless temperature
V	Molar volume
v_i	Atomic diffusion volume
x	Mole fraction
y	Argument of crossover function

Greek letters

α	Critical exponent
α_i	Coefficients of excess Onsager coefficient
$\tilde{\alpha}$	Onsager coefficient
β	Critical exponent
β_i	Coefficients of excess Onsager coefficient
$\tilde{\beta}$	Onsager coefficient
γ	Critical exponent
ν	Critical exponent
γ_i	Coefficients of excess Onsager coefficient
$\tilde{\gamma}$	Onsager coefficient

Δ	Difference
ϵ	Lennard–Jones potential parameter
η	Shear viscosity
λ	Thermal conductivity
μ	Chemical potential
ξ	Correlation length
σ	Lennard–Jones potential parameter
τ	Reduced temperature difference
Ω	Crossover function
$\Omega^{(2.2)}$	Collision integral
Ω_K	Kawasaki function
ρ	Molar density

Subscript

b	Background
c	Critical
ex	Excess function
nb	Normal boiling
x	Mixture properties
0	Dilute gas

Acknowledgements

The authors are indebted to D.G. Friend, H.J.M. Hanley, A. Laesecke, R.A. Perkins and H.M. Roder for valuable discussions and for providing the original files of the experimental data for methane + ethane mixtures. We are also indebted to M.A. Anisimov and J.V. Sengers for providing the manuscripts of their papers prior to publication and to J.C. Rainwater for constructive comments and interest in this work. One of us (S.B.K.) also would like to thank the Physical and Chemical Properties Division, National Institute of Standards and Technology for the opportunity to work as a Guest Researcher at NIST during the course of this research.

References

[1] L.D. Landau, E.M. Lifshitz, Statistical Physics, 3rd edn., Pergamon, New York, 1980.
[2] A.Z. Patashinskii, V.L. Pokrovskii, Fluctuation Theory of Phase Transitions, Pergamon, New York, 1979.
[3] E.E. Gorodetskii, M.S. Giterman, Sov. Phys. JETP 30 (1970) 348.
[4] L. Mistura, Nuovo Cimento 12B (1972) 35.
[5] L. Mistura, J. Chem. Phys. 62 (1975) 4571.
[6] A. Onuki, J. Low Temp. Phys. 61 (1985) 101.
[7] M.A. Anisimov, S.B. Kiselev, Int. J. Thermophys. 13 (1992) 873.
[8] S.B. Kiselev, V.D. Kulikov, Int. J. Thermophys. 15 (1994) 283.
[9] S.B. Kiselev, A.A. Povodyrev, in: A. Nagashima (Ed.), Proc. of the 4th Asian Thermophysical Properties Conference, Vol. 1, Keio University, Tokyo, 1995, p. 699.
[10] S.B. Kiselev, A.A. Povodyrev, High Temp. 34 (1996) 621.

[11] S.B. Kiselev, V.D. Kulikov, Int. J. Thermophys. 18 (1997) 1143.
[12] R. Folk, G. Moser, J. Low Temp. Phys. 99 (1995) 11.
[13] R. Folk, G. Moser, Int. J. Thermophys. 16 (1995) 1363.
[14] R. Folk, G. Moser, Phys. Rev. Lett. 75 (1995) 2706.
[15] J. Luettmer-Strathmann, J.V. Sengers, J. Chem. Phys. 104 (1996) 3026.
[16] S.B. Kiselev, Fluid Phase Equilibria 128 (1997) 1.
[17] S.B. Kiselev, J.C. Rainwater, Fluid Phase Equilibria, in press.
[18] L.D. Landau, E.M. Lifshitz, Hydrodynamics, Nauka, Moscow, 1988.
[19] R.A. Ferrell, Phys. Rev. Lett. 24 (1970) 1169.
[20] R. Perl, R.A. Ferrell, Phys. Rev. A 6 (1972) 2358.
[21] K. Kawasaki, in: C. Domb, M.S. Green (Eds.), Phase Transition and Critical Phenomena. Vol. 5A, Academic Press, New York, 1976. p. 165.
[22] K. Kawasaki, Ann. Phys. 61 (1970) 1.
[23] K. Kawasaki, Ann. Phys. 4 (1958) 430.
[24] K. Kawasaki, Ann. Phys. 4 (1958) 498.
[25] J.H. Ferziger, H.G. Kaper, Mathematical Theory of Transport Processes in Gases, North Holland, Amsterdam, 1972.
[26] J.V. Sengers, P.H. Keyes, Phys. Rev. Lett. 26 (1971) 70.
[27] G.A. Olchowy, J.V. Sengers, Int. J. Thermophys. 10 (1989) 417.
[28] L.I. Stiel, G. Thodes, AIChE J. 10 (1964) 26.
[29] E.N. Fuller, J.C. Giddings, J. Gas. Chromotogr. 3 (1965) 222.
[30] E.N. Fuller, P.D. Schettler, J.C. Giddings, Ind. Eng. Chem. 58 (1966) 18.
[31] A. Wassilijeva, Phys. Z. 5 (1894) 737.
[32] A.L. Lindsay, L.A. Bromley, Ind. Eng. Chem. 42 (1950) 1508.
[33] R.C. Reid, J.M. Prausnitz, B.E. Poling, The Properties of Gases and Liquids, McGraw-Hill, New York, 1987.
[34] V. Vesovik, W.A. Wakeham, G.A. Olchowy, J.V. Sengers, J.T.R. Watson, J. Millat, J. Phys. Chem. Ref. Data 19 (1990) 763.
[35] S. Hendl, J. Millat, E. Vogel, V. Vesovic, W.A. Wakeham, J. Luettmer-Strathmann, J.V. Sengers, M.J. Assael, Int. J. Thermophys. 15 (1994) 1.
[36] E.P. Sakonidou, H.R. van der Berg, C.A. ten Seldann, J.V. Sengers, J. Chem. Phys. 105 (1996) 10535.
[37] J. Millat, J.H. Dymond, Nieto de Castro (Eds.), Transport Properties of Fluids, IUPAC, Cambridge Univ. Press. London, 1996.
[38] J.O. Hirschfelder, C.F. Curtiss, R.B. Bird, Molecular Theory of Gases and Liquids, Wiley, New York, 1953.
[39] P.D. Neufeld, A.R. Janzen, R.A. Aziz, J. Chem. Phys. 57 (1972) 1100.
[40] P.M. Holland, H.J.M. Hanley, J. Phys. Chem. Ref. Data 8 (1979) 559.
[41] NIST Standard Reference Database 14, NIST Mixture Property Database, v9.08.
[42] J.V. Sengers, J.M.H. Levelt Sengers, in: C.A. Croxton (Ed.), Progress in Liquid Physics, Wiley, New York, 1978, p. 103.
[43] A. Michels, J.V. Sengers, P.S. van der Gulik, Physica 28 (1962) 1216.
[44] E.P. Sakonidou, Thermal conductivity of fluid mixtures in the critical region, PhD Thesis, Univ. of Amsterdam, 1996.
[45] R. Mostert, H.R. van der Berg, P.S. van der Gulik, J.V. Sengers, J. Chem. Phys. 92 (1990) 5454.
[46] R. Mostert, The thermal conductivity of ethane and its mixtures with carbon dioxide in the critical region, PhD Thesis, Univ. of Amsterdam, 1992.
[47] B. Le Niendre, Int. J. Heat Mass Transfer 15 (1972) 1.
[48] B. Le Niendre, R. Tufeu, P. Bury, J.V. Sengers, Ber. Bun. Phys. Chem. 77 (1973) 262.
[49] B. Le Niendre, R. Tufeu, P. Bury, P. Johannin, B. Vodar, in: C.Y. Ho, R.E. Taylor (Eds.), Proc. 8th Conf. on Thermal Conductivity, Plenum, New York, 1969, pp. 229–246.
[50] J.M. Lenoir, W.A. Junk, E.W. Comings, Chem. Eng. Prog. 49 (1953) 539.
[51] R.C. Prasad, J.E.S. Venart, Int. J. Thermophys. 5 (1984) 367.
[52] H.M. Roder, High Temp.–High Pressures 17 (1985) 453.
[53] J. Leffler, H.T. Gullinan, Ind. Eng. Chem. Fundam., 9 1970, pp. 84, 88.
[54] M.A. Lusis, G.A. Ratcliff, Can. J. Chem. Eng. 46 (1968) 385.
[55] J.E. Walther, Thermal Diffusion in Non-Ideal Gases. PhD Thesis, Univ. of Illinois, 1957.

[56] H.M. Roder, D.G. Friend, Experimental Thermal Conductivity Values for Mixtures of Methane and Ethane, Final Report NBSIR 85-3024, National Bureau of Standards, Boulder, CO, 1985.
[57] H.M. Roder, D.G. Friend, Int. J. Thermophys. 6 (1985) 607.
[58] D.G. Friend, H.M. Roder, Int. J. Thermophys. 8 (1987) 13.
[59] B.J. Ackerson, H.J.M. Hanley, J. Chem. Phys. 73 (1980) 3568.
[60] M.A. Anisimov, V.A. Agayan, A.A. Povodyrev, J.V. Sengers, Phys. Rev. E. submitted for publication.
[61] D.E. Diller, J. Chem. Eng. Data 29 (1984) 215.
[62] A.A. Povodyrev, G.X. Jin, S.B. Kiselev, J.V. Sengers, Int. J. Thermophys. 17 (1996) 906.
[63] E.P. Sakonidou, H.R. van den Berg, C.A. ten Seldam, J.V. Sengers, Phys. Rev. E., in press.
[64] R. Mostert, J.V. Sengers, Fluid Phase Equilibria 75 (1992) 235.